

N O T I C E

THIS DOCUMENT HAS BEEN REPRODUCED FROM
MICROFICHE. ALTHOUGH IT IS RECOGNIZED THAT
CERTAIN PORTIONS ARE ILLEGIBLE, IT IS BEING RELEASED
IN THE INTEREST OF MAKING AVAILABLE AS MUCH
INFORMATION AS POSSIBLE



Final
Report

April 15, 1980

Comet Nucleus Impact Probe Feasibility Study

(NASA-CR-152375) COMET NUCLEUS IMPACT PROBE
FEASIBILITY STUDY Final Report (Martin
Marietta Corp.) 69 p HC A04/MF A01 CSCL 22A

N80-26364

Unclas
G3/12 23982



MCR-80-1002
P.O. #A-71116B

Final
Report

April 15, 1980

COMET NUCLEUS IMPACT
PROBE FEASIBILITY STUDY

PREPARED BY: *Angelo J. Castro*
Angelo J. Castro
Technical Director

APPROVED: *Aubrey J. Butts*
Aubrey J. Butts
Program Manager

Prepared for
NASA-Ames Research Center

MARTIN MARIETTA CORPORATION
DENVER DIVISION
Denver, Colorado 80201

ACKNOWLEDGEMENTS

The following Martin Marietta Aerospace personnel participated in the performance of the is study and/or contributed to the preparation of the Final Report.

Fred Hopper
James Stevens
Michael Rossman
James Berry
Wang Foy
Howard Jong
Marion Grateluschen
Michael Leeds
Alan Rice
John Lear
Darlene Smith
Virgie Woods
James Jacobs
Alfred O. Britting, Jr.

TABLE OF CONTENTS

1.0	INTRODUCTION	1
2.0	EXPERIMENT REQUIREMENTS	2
2.1	Mission Requirements	2
2.2	Mission Operation Scenario	3
3.0	EXPERIMENT DESIGN CONCEPT	7
3.1	The CNIP	7
3.1.1	Acceleration Measurements	12
3.1.2	Date Conditioning and Telemetry Electronics	17
3.1.3	Telecommunication	20
3.1.4	Electrical Power	23
3.1.5	Mechanical Design	24
3.1.6	Propulsion	27
3.1.7	Umbilical Device	31
3.2	Experiment Base Station	31
4.0	Design Studies	34
4.1	Probe Structure Analysis	35
4.1.1	Nose Design	35
4.1.2	Forebody	35
4.1.3	Afterbody	37
4.1.4	Attitude Stability	38
4.2	Alternate CNIP Antenna Design	45
4.3	Power System Trade-Off Study	48

5.0	Management Data	53
5.1	Program Plan	53
5.2	Cost Analysis	57
	REFERENCE DOCUMENTS	60
	ACRONYMS	61
	APPENDIX	62

1.0 INTRODUCTION

This report presents the results of the Comet Nucleus Impact Probe Feasibility study directed by Ames Research Center P.O. A-71168. The tasks listed in purchase Requisition SPT-2546 Statement of Work have been fulfilled in this brief study and are reported herein as follows:

- 1.1 Section 2 presents a top-level listing of the CNIP Experiment requirements that were derived from the stated Experiment Objective.
- 1.2 Section 3 described a conceptual configuration from which a more definitized design can be developed. This concept shows the feasibility of engineering the experiment is possible and describes the candidate hardware.
- 1.3 Section 4 outlines the design studies that will be required in order to design the operating experiment.
- 1.4 Section 5 gives an overview of a program plan used to estimate a rough order of magnitude cost for the CNIP Experiment.

2.0 EXPERIMENT REQUIREMENTS

The objective of the experiment is "to measure probe impact signatures on the nucleus of Tempel 2 during the rendezvous phase of the mission. the signature is provided by means of a set of linear accelerometers constrained inside the probe".

The following requirements for the experiment were derived from this objective and/or assumed for this study.

2.1 Mission Requirements

- a. The S/C will come within 10 K meters of the nucleus of the Comet.
- b. The relative velocity between the Comet Nucleus and the S/C, at the time of CNIP Experiment operation, shall be 0 ± 10 m/s.
- c. Aiming shall be performed by the S/C and the scan platform, to the accuracy described in the referenced Comet Mission document. The range and relative velocity will be determined by the S/C altimeter as described in the referenced comet mission documents.
- d. The spacecraft RARA will be used to receive the transmitted data from the CNIP. The received data will be provided to the CNIP Experiment through a S/C interface.

e. Three probes shall impact the Comet Nucleus:

Probe Velocity: (1) at 50 m/s
(2) at 75 m/s

Impact Cone Angle: less than 10°

Probe Impact Mass: 1 Kg

f. Measurements

(2) Longitudinal Accelerometers: 0 - 2 K g
0 - 50 g
(1) Transverse Accelerometer: 0 - 2.5 g
(2) Temperature Measurement: 0° - 300° K

g. The Comet Mission description and the flight system description are presented in the referenced mission documents.

h. The CNIP Experiment shall impart a minute force impulse on the S/C during its operation by using an open tube launcher for the probes. The probe motor exhaust shall not impinge on, or contaminate, the S/C elements.

2.2 Mission Operation Scenario - The CNIP experiment will be delivered to the spacecraft and mounted on the scan platform such that it is covered by the thermal blanket, and the front end of the experiments launch tubes are pointed outward of the S/C. The launch and cruise of the S/C to the comet will be made with the CNIP experiment dormant. The S/C will provide the power to maintain a reasonable environment. The cruise to the comet may take some three years.

The CNIP Experiment will be activated when the S/C is within 10 K meters of the comet nucleus. The relative velocity between the comet and the S/C will be zero \pm 10 meters per second. Table 2.1 lists the functions required to perform the CNIP experiment mission.

The functions designated to the S/C all fall within the capabilities described in Reference 3. The CNIP will have the capability to interrupt the S/C Radar data and decide if it is unable to fire a probe (Function 13, Table 5.1). The S/C will contain the algorithm to locate the center of the nucleus and scan the platform to aim the CNIP Experiment. In function 14 of Table 5.1. The CNIP is freed of its restraining mechanism prior to firing the solid rocket.

The rocket motor burns for no more than 21 milliseconds and the CNIP leaves the tube with a forward velocity of 50 to 75 m/sec and a spin velocity of about 100 radians per second. During the 133 to 200 seconds of travel to the nucleus the CNIP will continuously transmit acceleration and temperature data. These measurements will be transmitted to the S/C during impact into the nucleus and continue to transmit for some 60 minutes. The data from the CNIP is received by the S/C RARA and handed to the CNIP experiment. The data is decoded and digitized by the experiment and sent to the S/C CDS for transmission to earth.

Each of the three probes may be fired in an automatic sequence or singularly upon command from the earth.

TABLE 2.1

OPERATING FUNCTIONS

1. Energize CNIP Experiment
2. Locate Comet Nucleus (S/C - Radar)
3. Maintain CNIP Experiment Environment
4. Determine Nucleus Range (S/C - Radar)
5. Determine S/C - Nucleus Relative Velocity (S/C - Radar)
6. Slew Platform (S/C - CDS)
7. Command CNIP Experiment (S/C - CDS)
8. Receive Cmd and Execute
9. Calibrate and Adjust CNIP Experiment
10. Measure Experiment Temperature
11. S/C Provide Experiment Proceed Cmd (S/C - CDS)
12. Receive Cmd and Execute
13. Determine if Conditions are OK to Fire
14. Sequence Experiment, Activate Securing Mechanism and Fire Motor
15. Accelerate and Spin Probe
16. Burn-out Motor In-tube
17. Deploy Fins
18. Maintain Stability during Free Flight
19. Collect Acceleration Data
20. Collect Temperature Data
21. Condition Data
22. Transmit Data to S/C RARA
23. Receive Data on S/C (S/C - RARA)
24. Send Data to CNIP Experiment (S/C - RARA)
25. Accept, Process and Store Data
26. Impact Nucleus
27. Separate Afterbody
28. Maintain Mechanical and Electrical Integrity within Probe
29. Collect Acceleration Data for 3 Hours
30. Collect Temperature Data for 3 Hours

TABLE 2.1 (continued)

31. Transmit Data S/C RARA for 3 Hours
32. Receive Data on S/C for 3 Hours (S/C RARA)
33. Send Data to CNIP Experiment (S/C - RARA)
34. Accept, Process and Store Data
35. Provide Digital Data to S/C CD'S
36. Transmit Data to Earth
37. Earth Receive, Process and Decide
38. Earth Command S/C
39. Repeat Functions 1 through 38 for each Probe

3.0 DESIGN CONCEPT

The CNIP Experiment is conceived as a single unit that is mounted on the scan platform of the Comet Spacecraft. Figure 3.1 is a sketch of the Experiment Base Station which contains the elements shown in the block diagram Figure 3.2. The CNIP Experiment Base Station contains three 120 cm long launch tubes that are loaded with three probes (CNIP's). Each CNIP weighs about one kilogram and contains the hardware to sense axial acceleration, transverse acceleration and the temperature of the nose. The CNIP transmits these measurements on S-Band, 2200 MHz, carrier to the (RARA) antenna on the spacecraft. The CNIP Experiment Base Station electronics accepts the signal and contains the electronics to discriminate each measurement, convert the data to digital format, and then transfers the data to the spacecraft's CDS.

This conceptual design has the physical characteristics listed in Table 3.1. These characteristics were developed as a straw-man configuration for this feasibility study and a more detailed design will have to be developed from the science studies and design analyses that are discussed in Section 4.0.

3.1 The CNIP - The Impact probe is sketched in Figure 3.3. The nose is a simple cone shape made of hard steel and ballast to concentrate the probe weight. Imbedded within the nose material are the temperature sensors and mounted onto the nose material are the axial accelerometers. Locating these sensors in direct contact with the nose should maximize their direct measurement of the deceleration and boring temperature. The forebody of the probe also contains the power source, data handling and umbilical device. The forebody can continue to travel into the comet nucleus for 10 meters beyond the impact probe afterbody. The afterbody is stopped at the

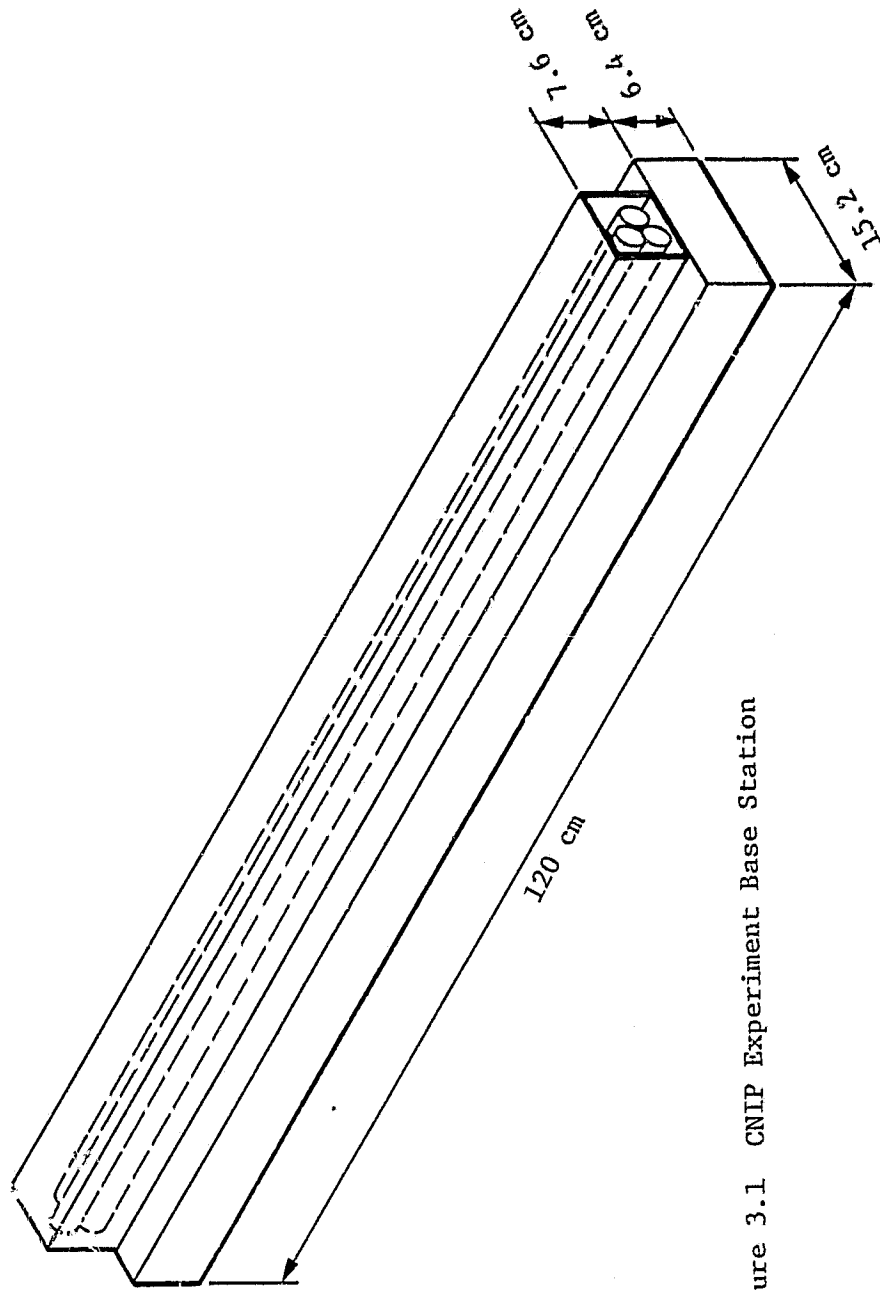


Figure 3.1 CNIP Experiment Base Station

CNIP

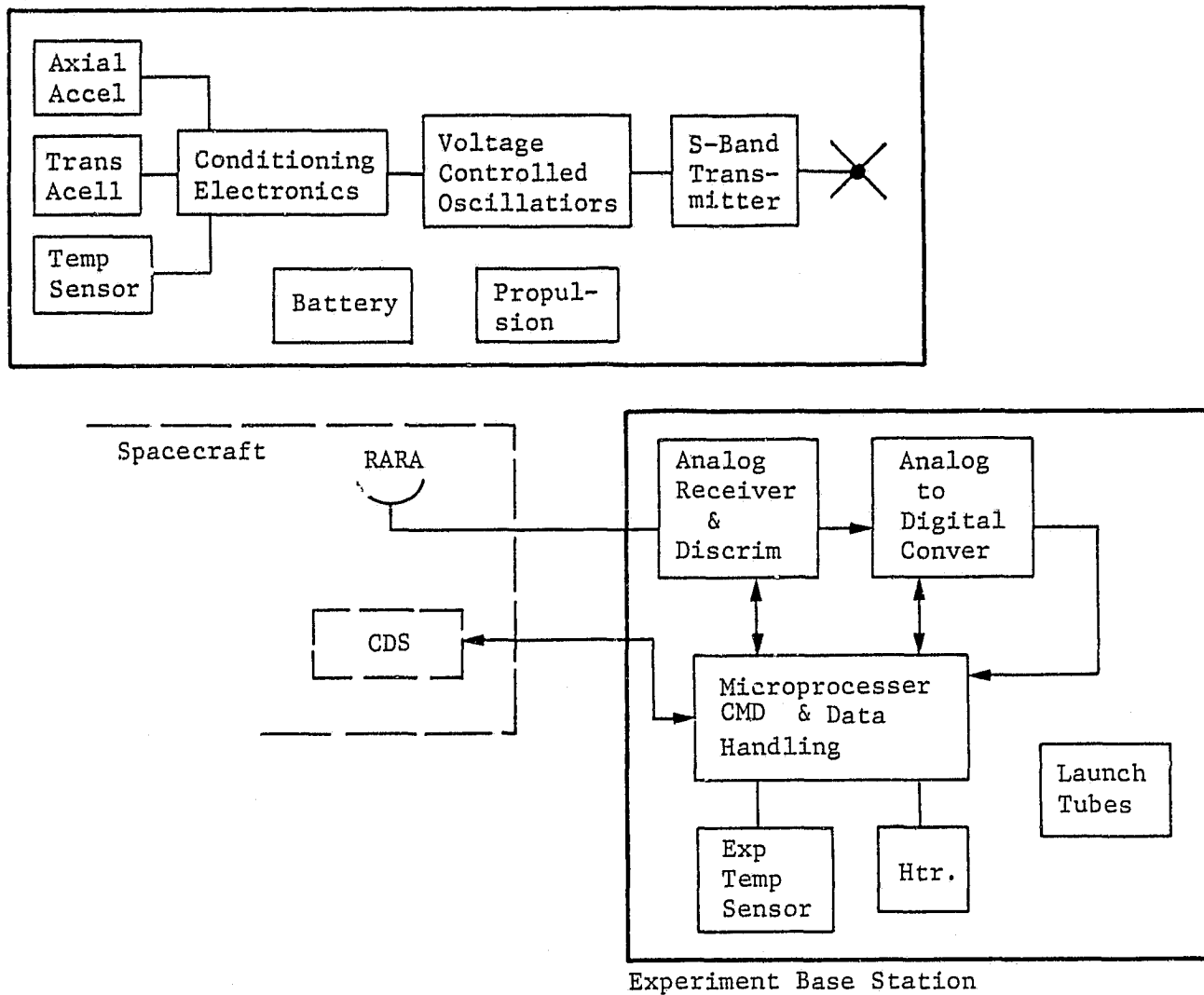


Figure 3.2 CNIP Experiment Block Diagram

TABLE 3-1

CNIP EXPERIMENT CHARACTERISTICS

Experiment Base Station (Figure 3.1)

Weight (with 3 CNIPs loaded)		5.2 Kg
Volume	Total	.019 m ³
	Launch Tube Box	.007 m ³
	Base Station Electronics	.012 m ³
Power (28 V from S/C)		5.0 Watt
Thermal Power		1.0 Watt

CNIP - (Figure 3.3)

Number per experiment		3
Length		40 cm
Diameter		2.54 cm
Weight		824 gm
Case Material		Steel
Nose Type		Cone
Nose Material		Steel
cg at impact (assume w/o Motor)		15 cm from nose tip
Weight at impact (assume w/o motor case)		739 gm

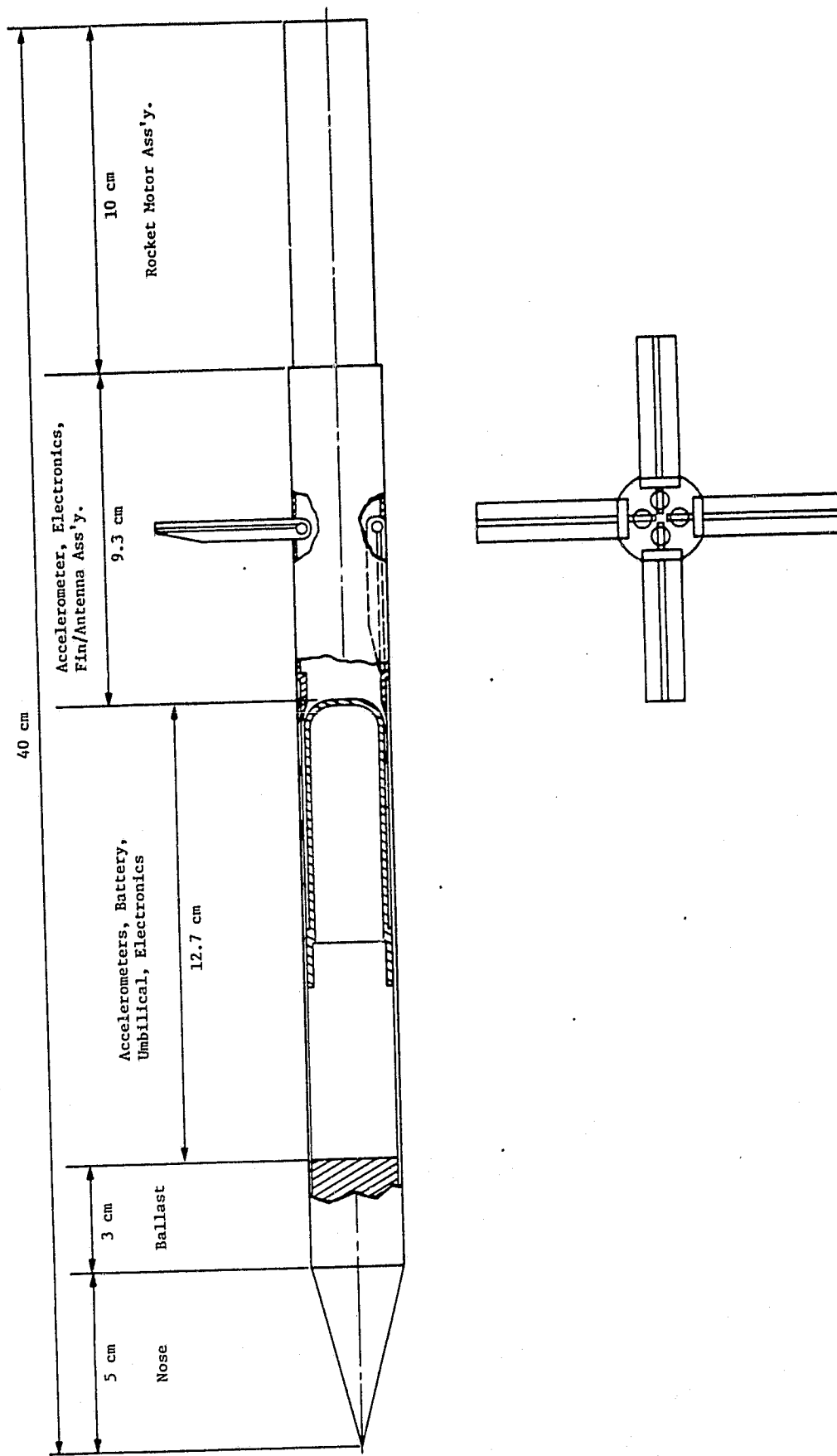


Figure 3.3 Comet Nucleus Impact Probe

nucleus surface by four brake-fins, such as are diagrammed in Figure 3.3. This conceptual design used a brake-fin length of approximately 1.5 probe diameters. The afterbody also contains the telecommunication subsystem, the transverse accelerometer with its amplifier, the afterbody brake-fin mechanism and the Solid Rocket Motor. Figure 3.4 shows the hardware elements that makeup the CNIP. These probe elements are described in the following paragraphs:

3.1.1 CNIP Probe Acceleration Measurements

3.1.1.1 Axial Accelerations - Two accelerometers having different ranges are required to cover the range of decelerations to be expected as the probe enters the nucleus of the comet. A high range instrument (0-2000g) with high frequency response is needed to measure the impact, assuming a frozen rock nucleus. A lower range instrument (0-50g) with high resolution will detect the probe impacts with small particles.

The following instruments were selected for longitudinal measurements:

High Range: Endevco Model 2272M1.5 the instrument characteristics are show below:

Sensitivity, pC/g	13
Capacitance, pF	2 700
Frequency Response, Hz	2-7,000
Mounted Resonance, Hz	37,000
Amplitude Range, g	0 to 2,000
Size, inches	.625 hex x .78H
Weight, grams	27

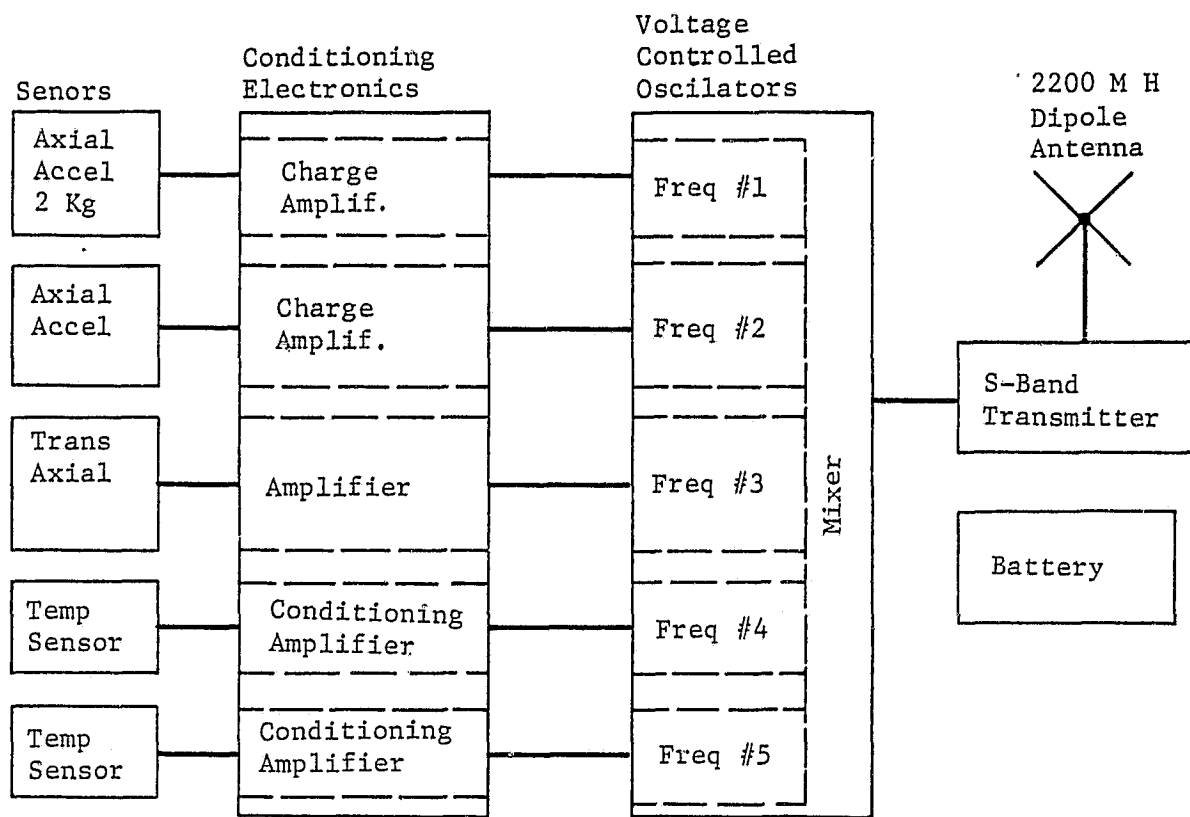


Figure 3.4 CNIP Hardware Block Diagram

Low range: PCE Piezatronics, Inc. Model 308B

Range (for \pm 5V output)	g	\pm 50
Resolution	g	0.002
Sensitivity (\pm 2%)	mV/g	100
Resonant Frequency (mounted)	Hz	25000
Frequency Range (\pm 5%)	Hz	1 to 3000
Linearity	%	1
Output Impedance	ohms	100
Overload Recovery	Microsec	10
Transverse Sensitivity (max)	%	7
Strain Sensitivity	g/min/in	.05
Temperature Coefficient	% $^{\circ}$ F	0.03
Temperature Range	$^{\circ}$ F	-100 to + 250
Vibration & Shock (protected)	g	500/5000
Size (dia. x height)	in	0.75 x 1.4
Weight	gram	87
Seal	epoxy	
Case Material	Stainless Steel	
Excitation (thru C.C. Diode)	VDC	+18 to 24
Excitation Current	mA	2 to 20

3.1.1.2 Transverse Acceleration - The measurement of transverse probe body motions requires a transducer of high sensitivity and high resolution, but not high accelerations range. In order to detect the small accelerations due to coning motion of the probe, the transducer should be as far from the probe C.G. as possible. For a 10 degree coning angle and a coning rate of 0.6 rad/sec, an accelerometer located 20 cm from the probe C.G., would sense an acceleration of 0.00127 g. The transducer should have a resolution of 0.0005 g or better.

The center of mass of the seismic mass of the accelerometer must be located very nearly on the axis of the probe to minimize the effect the spinning of the probe. For example, if the seismic mass were displaced from the probe axis by 1 mm, the transducer would indicate a steady state acceleration 0.65 g. The body accelerations on the order of 0.001 g would be superimposed on this steady state value.

A candidate sensor for the transverse acceleration measurement is a PCP Piezatronics, Inc. Model 308A02. The range of this instrument 2.5g and the resolution is 0.005g. The instrument has built-in electronics. Power requirement is 2 to 20 ma at 18-24 VDC.

The instrument characteristics are shown below:

PCB Piezatronics Model 303A02

Range	\pm g	2.5
Sensitivity (\pm 2%)	Millivolts/g	1000
Resolution	g	.0005
Resonant Frequency	Hz	25,000
Frequency Range (\pm 5%)	Hz	1 to 3000
Amplitude Linearity	%	1
Transverse Sensitivity	%	7
Temperature Coefficient	% oF	.03
Temperature Range (6)	oF	-65+250
Vibration (Max)	\pm g	100
Shock (Max.)	g	200
Size (Hex. X Height)	in	3/4 x 1.3
Weight	gram	87

It should be noted that this instrument cannot be fitted transversely into a 1.0 inch diameter cylinder. An inside diameter of 1.5 inches would be required as a minimum. If the seismic mass were not located on the geometric center of the transducer case, the transducer would have to be shifted along its sensitive axis relative to the probe center line in order to place the seismic mass on the probe spin axis. This would necessitate a still larger probe diameter. This is also true of other transducers having suitable performance characteristics to meet the transverse acceleration measurement requirement.

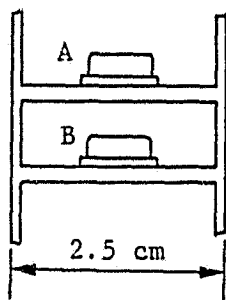
Application of this accelerometer in the final design will require either a large diameter CNIP or a custom repackage by the manufacturer.

3.1.2 Data Conditioning and Telemetry Electronics

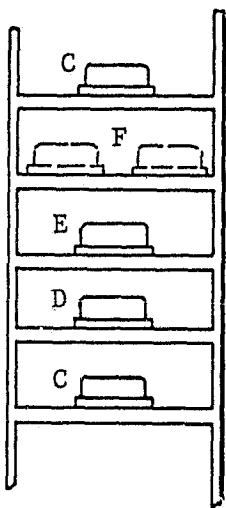
The electronics hardware for this straw-man CNIP design is designated in Figure 3.4. The hardware consists a five-channel system that conditions the signals from the three accelerometers and the two temperature sensors. It is made up of three charge amplifiers, two conditioning amplifiers, five voltage-controlled amplifiers, a five channel mixer and a 200 milliwatt S-Band transmitter.

Physical location of the electronics is divided into the forebody and afterbody sections. The afterbody section was designated to contain the high frequency components so that the umbilical cable would only carry d.c. voltages.

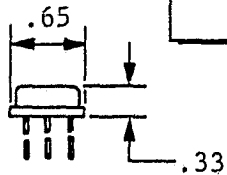
A five channel system can be hybridized using a series of circular printed circuit boards, with each board supporting a standard TO-8 package. The physical layout conceived is shown in Figure 3.5 and the contents of each section is shown therein. The detail design of these sections can be made to provide the structural support to allow the package to tolerate the high impact force. The orientation of the TO-8 package can also be optimized in order to minimize the stress on the components of the package.



Forebody



Afterbody



<u>TO-8 PACKAGE</u>	<u>CONTENTS</u>
A	Two-channel charge Amplifier (axial accel.)
B	Two-channel conditioning Amplifiers (temp sensors)
C	Two Channel Voltage controlled oscillator
D	Two channel Voltage Controlled oscillator
E	Mixer
F	S-Band Transmitter
G	One Voltage controlled Oscillator , one conditioning Amplifier (Transaxial Accel.)

Figure 3.5
Electronic Package Concept

3.1.2.1 Charge Amplifier - This preamplifier is a low noise, low power, wideband charge amplifier. It is biased by 15 volts and has power requirements of approximately 20 mW per channel. Each channel consists, of 5 bipolar transistors, 1 FET (input), 12 thick-film resistors, and 7 capacitors for a total of 13 chips. Hybrids are fabricated on alumina substrates with thick-film gold conductor traces. Aluminum ultrasonic bonded and gold thermocompression bonded wiring technology is employed. TO-8 packages are hermetically sealed using seam welding techniques. Amplifiers are active trimmable for gain and waveform adjustments during assembly.

3.1.2.2 Conditioning Amplifier - This amplifier will be similar to the charge amplifier with respect to bias, power, component content, and construction techniques.

3.1.2.3 Voltage-Controlled Oscillator - This Colpitts oscillator is varactor-tuned with a varactor diode acting as a voltage-controlled capacitor for frequency tuning. It is biased by 15 volts and has power requirements of approximately 20 mW per channel. Each channel consists of 1 transistor, 1 varactor diode, 1 coil, 3 thin film resistors, and 2 capacitors for a total of 5 chips. Hybrids are fabricated on alumina substrates with thin film gold conductor traces. Wiring and package sealing technology is as described for charge amplifiers.

3.1.2.4 Mixer - This mixer is a broadband, high isolation signal mixer and frequency up converter. It is biased by 15 volts and has power requirements of approximately 100 mW. A typical circuit consists of 5 transistor, 2 choke coils, 4 thin film resistors, and 5 capacitors. This circuit requires special fabrication techniques and material due to the frequencies involved. Thin film microstripline would be used on alumina or quartz substrates to provide proper impedance matching and circuit conductors. Wiring and package sealing technology would be as described for charge amplifiers with the exception that beamlead transistors might have to be employed.

3.1.2.5 S-Band Transmitter - This circuit may be purchased as a hybrid from outside sources or may be fabricated internally. It consists primarily of a wideband, RF amplifier typically made up of 4 transistors, 8 thin film resistors, and 5 capacitors. Thin film technology, wiring, and package sealing would be as described for the mixer hybrid biasing is at 15 volts with power capability up to 500 mW. Ultimately, power requirements will depend on the range to the spacecraft, type of antenna used, and other transmission variables.

3.1.3 CNIP Telecommunication - Figure 3.6 diagrams the signal circuit from the transmitter to the antenna and Figure 3.7 shows the configuration of the antenna. The antenna design, for the 2200 MHz, is a 1/2 wavelength dipole of 6.8 cm. Figure 3.8 sketches the antenna on the Brake-Fin and Figure 3.9 shows the beam pattern. The gain is 1.5 to 3 db and the bandwidth design would be sufficient to accommodate the five channels frequency spread around the 2200 Mh. The design of the antenna can be accommodated with the size of the fins and the body diameter to provide the 6.8 cm half wavelength required.

The obvious difficulties with this design are twofold:

- 1) The brake-fins may penetrate into the comet nucleus mass and cover the antenna. This would prevent radiation of the signal.
- 2) The impact shock can cause distortion or loss of the antenna.

In section 4.0 alternate antenna designs are briefly discussed.

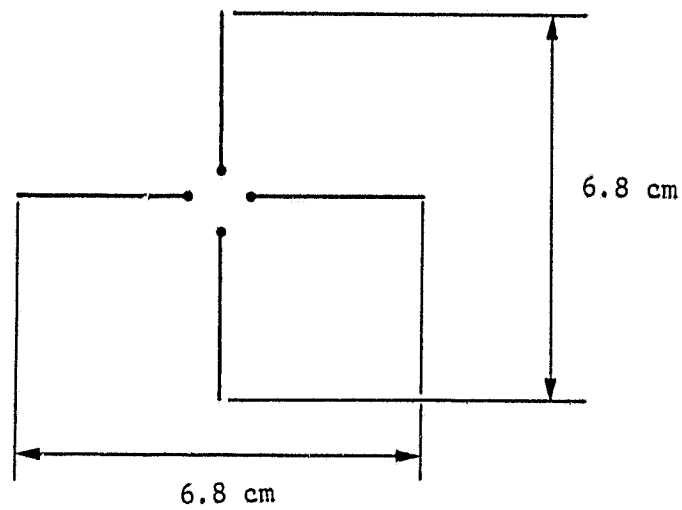


Figure 3.7 $\frac{1}{2}$ Wavelength, Cross-dipole Antenna

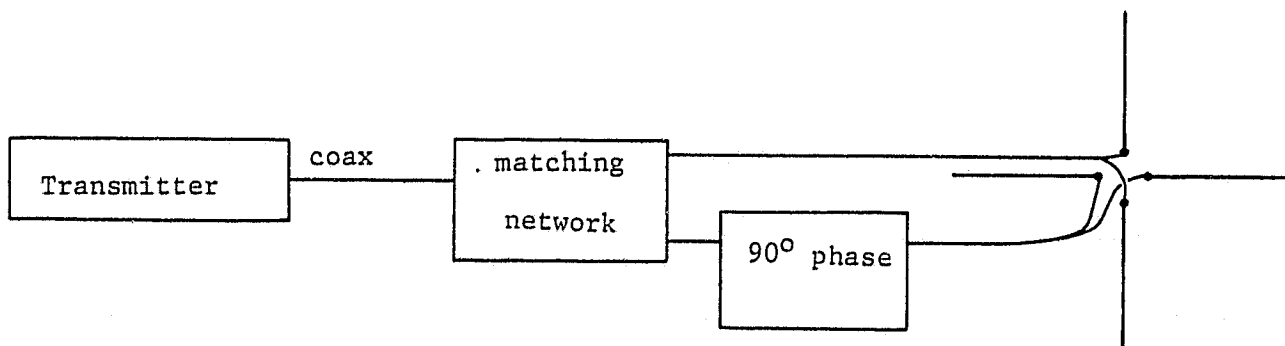


Figure 3.6 Signal Path-transmitter to Antenna

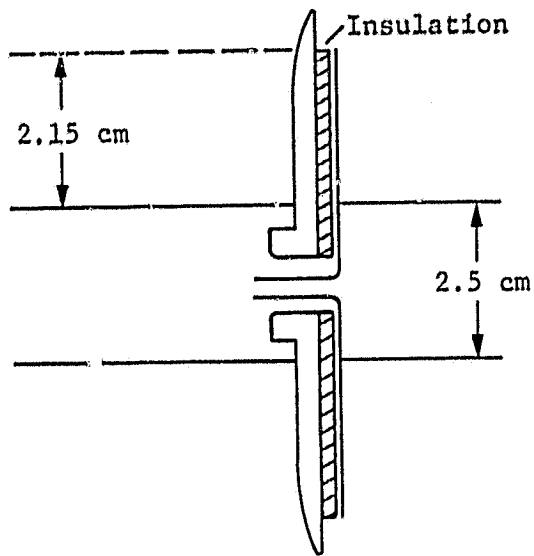


Figure 3.8 Antenna on Brake - Fin

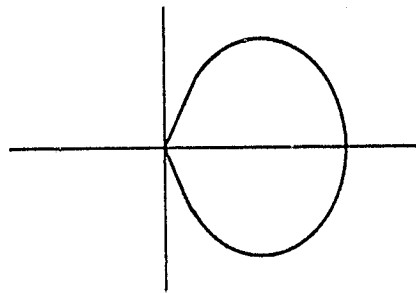


Figure 3.9 Cross - Dipole Antenna Beam Pattern

3.1.4 Electrical Power - The CNIP will require a power source that can meet the requirements of Table 3.2. A set of five lithium thionyl chloride cells (similar to Power Conversion, Inc. #44-10) was chosen to meet these requirements. This battery is capable of delivering 0.5 ampere-hours and, assuming an 8% loss at end-of-life, yields an end-of-life capacity of 0.46 ampere-hours. This is well above the required operating capacity of 0.3 ampere-hours. The characteristic of the battery is given below:

Type Cell	LiSOCl ₂
Cells Required	5
Diameter	2.54 cm
Length	7.62 cm
Weight	0.24 lbs
Capacity	0.5 Ampere-hours

A trade-off analysis for the power system is presented in Section 4.0.

TABLE 3.2: Battery Imposed Requirements

Max Dormant	2.54 cm
Document Life	3 years
Storage Temperature	100-300°K
Operating Period	1 hr.
Operating Voltage	15.0 \pm 3 Vdc
Operating Current	.3 Amp. (Steady)
Impact Shock	2000 g

3.1.5 CNIP Mechanical Design - The design goal for the physical characteristics of the impact probe is to penetrate the nucleus with a weight of 1000 grams with the cg of the probe located as close to the nose as possible.

The straw-man design for the CNIP (Figure 3.3) is sectioned as shown in Figure 3.10. The center-of-gravity lies at 17.2 cm from the nose. The weight breakdown for each section is given in Table 3.5.

The weight of 824 gm falls short of the goal of 1000 gms. the weight could be increased by using a heavier material for the ballast or by adding to the length (approx 3.3 cm) and/or increase the diameter of the probe. The use of gold in the nose and ballast could increase that portion's weight by a factor of about 2.4 and get the weight above the 1000 gram goal and move the cg further forward.

The-center-of-mass could also be moved forward by separating the rocket motor case from the probe prior to impacting the nucleus.

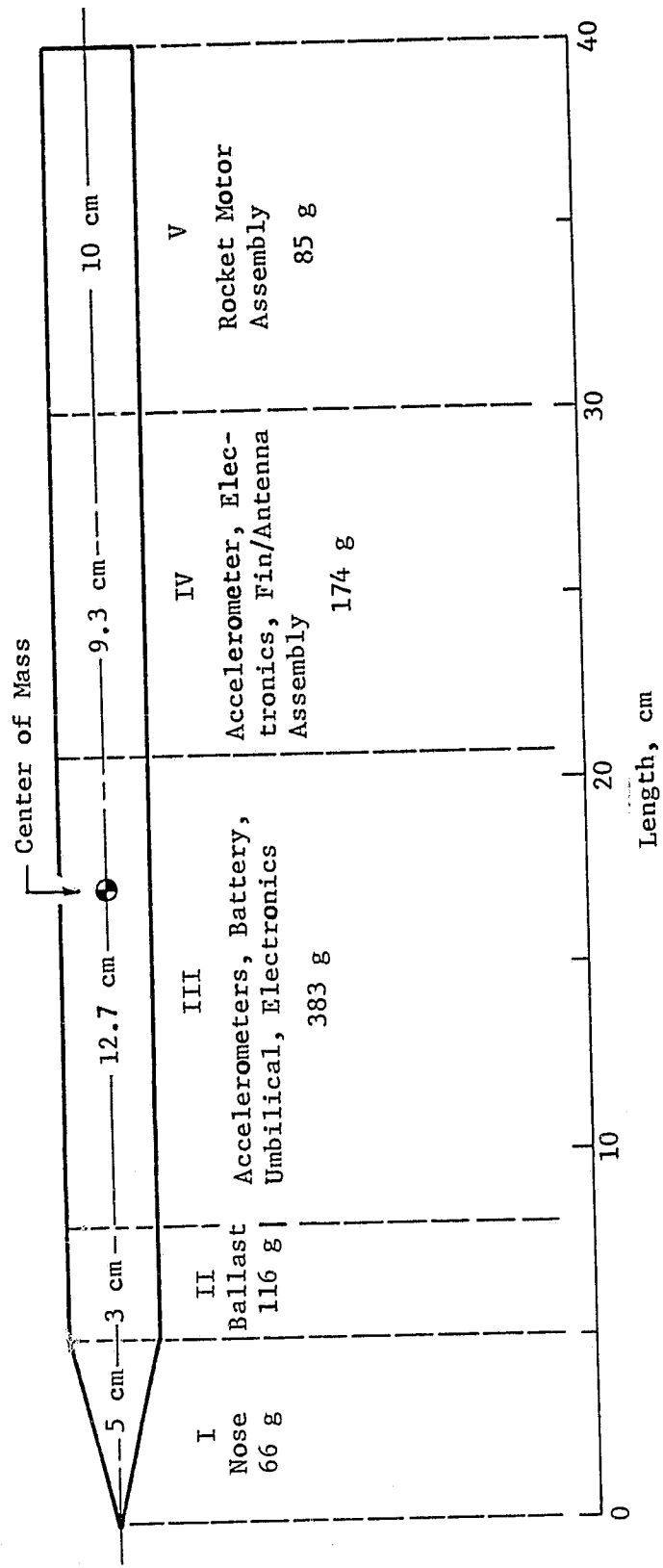


Figure 3.10 CNIP Mass Sectioning

Table 3.5

CNIP MASS ANALYSIS

Section (Fig 3.10)		<u>Weight</u> (grams)
I.	Conical Steel Nose, $\frac{L}{D} = 2$	66
II.	Steel Ballast Section	116
III.	Sensor/Electronic Section:	383
	High range accel.	27
	Low range accel.	87
	Battery	109
	Umbilical Cable, Electronics	50
	<u>1"</u> Steel Tube	110
	16	
IV.	Afterbody	174
	Lateral Accelerometer	40
	Electronics, fin/assembly	53
	<u>1"</u> Steel Tube	81
V.	Rocket Motor Assy.	<u>85</u>
TOTAL WEIGHT		824 grams

3.1.6 CNIP Propulsion - The key requirements and constraints affecting the SRM (Solid Rocket Motor) design are as follows:

- o CNIP Mass at Impact 1000 grams
- o Required velocity increment (ΔV) of 50 to 75 mps
- o Maximum outside diameter of 2.5 cm
- o Maximum burn time of approximately 20 ms
(to insure a complete burn within the launcher tube)

Based upon these requirements and an assumed specific impulse of 2160 Ns/Kg ($220 \text{ lb}_{f-s}/\text{lb}_m$) the following propellant mass and total impulse requirements were identified utilizing the ideal velocity equation:

	<u>V, m/s</u>	
	<u>50</u>	<u>75</u>
Propellant, gm	23.4	35.4
Total Impulse, Ns	50.6	76.3
Burning Time, S	.0141	.0213
Mean Thrust, N	3580	3580

In computing the above, a squarewave shown in Figure 3.11 was assumed for the thrust. Peak acceleration will be about 20% higher than the tabulated value.

Table 3.6 shows the results of a survey of small solid rocket motors produced over the last 20 years. The survey was made using the Rocket Motor Manual, CPIA/M1, Chemical Propulsion Information Agency, the John Hopkins University. While the document is classified, each of the motors shown in the table are unclassified. For further information on any SRM, the first column of the table lists the CPIA Unit Number which identifies each specific motor in the manual.

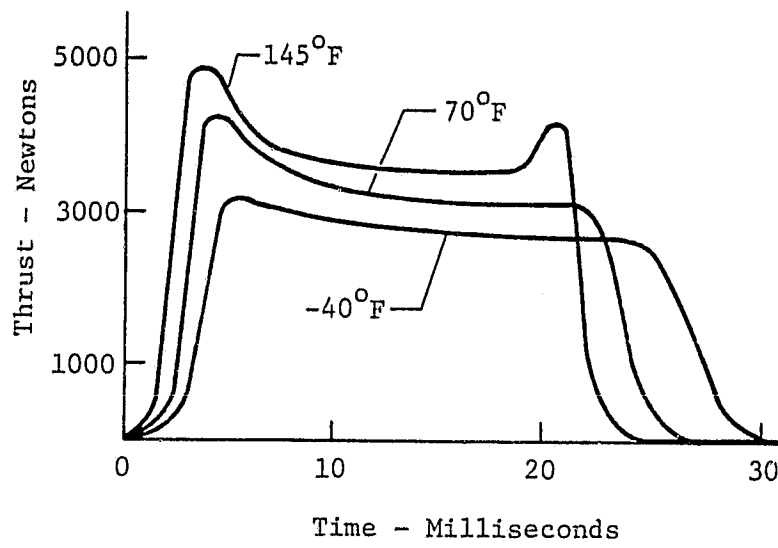


Figure 3.11 SRM Thrust Characteristics

TABLE 3.6 - SOLID ROCKET MOTORS

UNIT NO.	LEN. (CM)	MAX. DIA. (CM)	INERT MASS (GRAM)	PROP. MASS (GRAM)	MASS FRACTION	BURN TIME (S)	AVE TOTAL THRUST (N)	TOTAL IMPULSE (NS)	SPECIFIC IMPULSE (Ns/Kg)
331	27.2	4.8	2690	254	0.09	0.46	1100	507	2000
338	17.3	3.9	267	97	0.27	1.07	170	184	1900
397	21.5	6.5	295	62	0.17	0.012	12310	140	2300
406	16.5	3.9	270	97	0.26	1.07	203	220	2275
407	24.8	3.9	420	59	0.12	0.72	172	130	2210
499	38.7	7.4	1175	948	0.45	0.68	2180	2020	2135
502	18.8	5.9	303	163	0.35	0.32	1020	371	2275
516	7.5	3.0	120	23	0.16	0.105	420	50	2140
517	8.7	3.7	197	48	0.20	0.106	854	100	2080
520	3.6	2.9	14	9	0.39	0.021	-	16	1885
543	21.0	4.3	525	77	0.13	0.23	610	150	1970
544	8.6	3.7	159	45	0.22	0.111	770	98	2170

The fundamental requirement on the propulsion system is that the probes be accelerated to their design nucleus impact velocities in such a manner that thrust is terminated by the time they reach the forward end of the firing tubes. This implies the choice of a motor which burns almost explosively. Upon ignition the thrust rises rapidly to a peak about 20% greater than mean, then holds nearly constant to burnout. This provides the desired ΔV over approximately 21 milliseconds. The thrust-time history is fairly sensitive to ambient temperature, indicating a need for temperature control before firing the probe launch. The 75 m/s motor is to be used for the lower velocity probes, with a reduced propellant charge.

The SRM has an unfavorable mass ratio, with one having a dry weight of about 170 grams and carrying 35 grams of propellant. The specific impulse is approximated at 220 sec. The possibility of somehow jettisoning the exhausted motor after launch should be investigated for the final design.

Spin stabilization (see Section 4.0) imposes a requirement that during motor burn the probe attain an angular acceleration. This is most easily provided by fins or buckets, which will literally deflect a small fraction of the outer portion of the exhaust stream. As an example, consider the 75 m/s probe. If 5% of the exhaust gas is thus deflected laterally 10° , an angular velocity of 82 rad/sec would be imparted by burnout. This superficial analysis, indicates that it is feasible to obtain spin rates in the range of 50 - 100 rad/sec (500 - 1000 rpm).

Since this spin is imparted over a very short time interval ($\approx .02$ sec), rather high angular accelerations are experienced by the probe. Mean values are shown below vs spin rate, for the 75 m/s probe, with peak values about 20% higher.

Mean Linear Acceleration	Mean Angular Acceleration, rad/sec ²		
	20 rad/sec	60 rad/sec	100 rad/sec
350 g's	900	2800	4700

Acceleration levels are about the same for the 50 m/s probe, but give rise to proportionally lower spin rates. (This assumes approximately the same thrust level over a 33% shorter burn time.

The motor thrust characteristic, shown in Figure 3.11 implies a thrust tailoff on the order of 1% of the total impulse, part of which may be imparted after the probe has left the launch tube. If so, because of thrust misalignment, a disturbing moment is imparted over such a short time interval (e.g., 2 milliseconds, during which the probe rotates less than 3°) that it can be regarded as a pure moment impulse. The effect of this impulse in the attitude stability analysis in Section 4.0.

3.1.7 Umbilical Cable - The umbilical cable device that is indicated in Figure 3.3 was scaled from the work done by Ames Research Center. Based on that test data results a cylindrical mandrel was assumed for this study. The less than one inch diameter is smaller than anything tested in the ARC report. For the CNIP requirement, a 4.5 cm wide by 6.4 cm long cylinder is need to hold the 10 meters of six-strand cable. Since space is at a premium in this CNIP design the inside of the cylinder will contain some probe electronics. A cable length of less than 10 meters could shorten the cylinder and allow for better utility of the space in the Probe. Referring to Figure 4.1, the penetration into a frozen-rock nucleus could permit a much shorter cable length to be used. Design studies and umbilical tests will be required during design development of the CNIP.

3.2 Experiment Base Station - The Base Station is outlined in Figure 3.1 and Figure 3.12 is a block diagram of its elements. The functions of the base station are to, (1) provide the housing and environment for the launching of the CNIP, (2) provide the electronics to interface with the S/C, and (3) receive and process the data from the CNIP and transfer this data, in proper format to the S/C command and data system.

The physical characteristics of the experiment base station are given in Table 3.1.

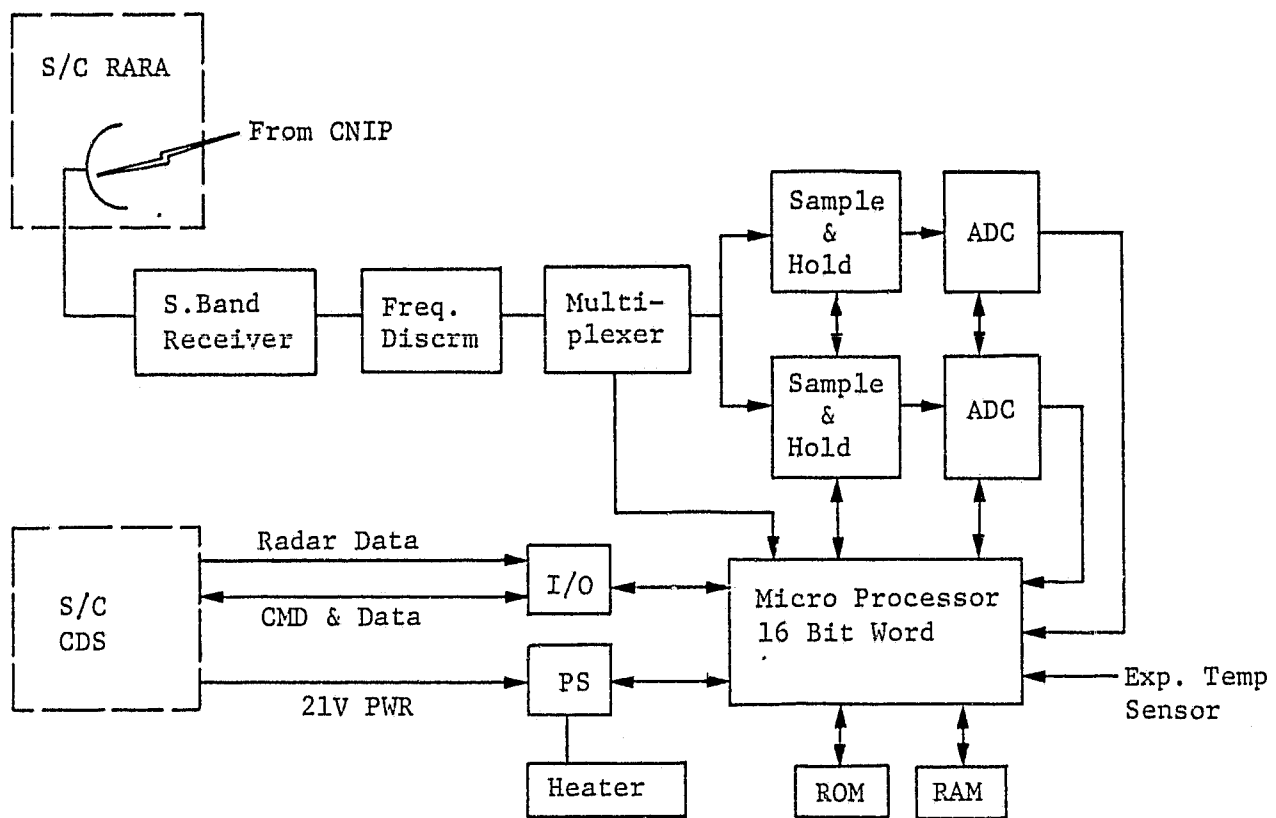


Figure 3.12 CNIP Experiment Base Station Block Diagram

The block diagram, Figure 3.12, shows the signal flow and the functions that are required to process the CNIP data. The analog signal is received by the S/C RARA and sent to the experiment. The Experiment Base Station has a S-Band receiver and a Frequency Discriminator to separate the five frequencies. The Multiplexer is controlled by the computer and it inturn selects each channel to be sampled. There are shown two sets of sample/hold analog-to-digital conversion circuits. The concept of using more than one circuit is to allow the computer to select the sensor during various phases of the CNIP mission. For instance, the low range axial accelerometer and the transaxial accelerometer would be sampled at the highest rate possible during the transient time to the nucleus. The high range axial accelerometer could be sampled at the highest rate during the CNIP penetration into the nucleus. The temperature sensor sampling can always be relegated to a lower sampling rate since changes in temperature can be anticipated to change more linearly in a positive or negative direction. The analog-to-digital conversion can easily be performed in the order of one microsecond, or better, for an eight bit word. Therefore, each circuit can reproduce the analog signal to a granularity of 10^6 data points per second. Science study and design analysis may show that such granularity is not warranted, and, therefore, either one circuit would be sufficient or a slower A/D converter can be chosen.

The computer will be capable of performing the function of storing the digital data and transferring the data to the S/C data system. It will also be capable of maintaining the temperature of the launch tube prior to firing the CNIP.

The electronics in the Base Station can be housed in the $11,673 \text{ cm}^3$ volume (120 x 6.4 x 15.5 cm), shown in Figure 1, below the launch tubes. This much volume can allow the design to use off-the-shelf computer cards rather than custom building the computer. However, if the experiment weight or volume is required to be minimized, the electronics can be built into a much smaller volume.

4.0 DESIGN STUDIES

In the course of performing this feasibility study a number of very quick, quantitative type analyses were performed. These analyses are documented in this section. These analyses made us aware of science and design studies that should be performed in the process of developing a detail design for the CNIP experiment. The following studies are recommended:

- A. Comet Nucleus Model
- B. CNIP Nose Shape
- C. CNIP Impact Weight
- D. CNIP Nose Material
- E. CNIP Depth of Penetration
- F. Impact Force Determination
- G. Impact Force Characteristic
- H. Attitude Stability Analysis
- I. Impact Coning Allowance
- J. Transverse Acceleration Requirement
- K. Axial Acceleration Requirements
- L. Afterbody Braking Study
- M. Propulsion Trade Off
- N. Rocket Motor Detachments Methods
- O. CNIP Antenna Alternates
- P. Umbilical Cable Design & Miniaturization
- Q. Battery Design
- R. Hybrid Electronics Design

4.1 Probe Structure Analysis

4.1.1. Nose Design - A conical nose with an L/D of 2 was arbitrarily chosen for the study. The penetration characteristics of various nose shapes can be measured by a coefficient N, which varies from .82 for a cone of L/D = 1 to 1.33 for a cone of L/D = 3, with various ogives and other shapes lying in between (see Reference 1). N for the selected cone of L/D = 2 is approximately 1.1. The differences are not of great importance in a preliminary design although the subject must be studied during any final design activities. Steel was chosen as the nose material since it was used by earlier penetration investigations documented in the referenced reports.

4.1.2 Forebody - Depth of penetration and resulting level of deceleration experienced by a probe can be predicted using the equations and data of Ref. 1. These equations take into account nose shape, material being penetrated, and probe velocity; and assume that the probe impacts with its longitudinal axis closely aligned with its velocity vector, and does not deform during penetration. Uncertainty of the estimates is in the order of $\pm 40\%$.

Figures 4.1 and 4.2 show such data for the probes defined in this study. The maximum deceleration force that various probe tube walls can withstand, without deformation, are listed in the following chart. These estimates assume a nose/ballast weight of 400 grams (including components bearing direct thereon), and are based on the stress experienced by the tubing just aft of that section.

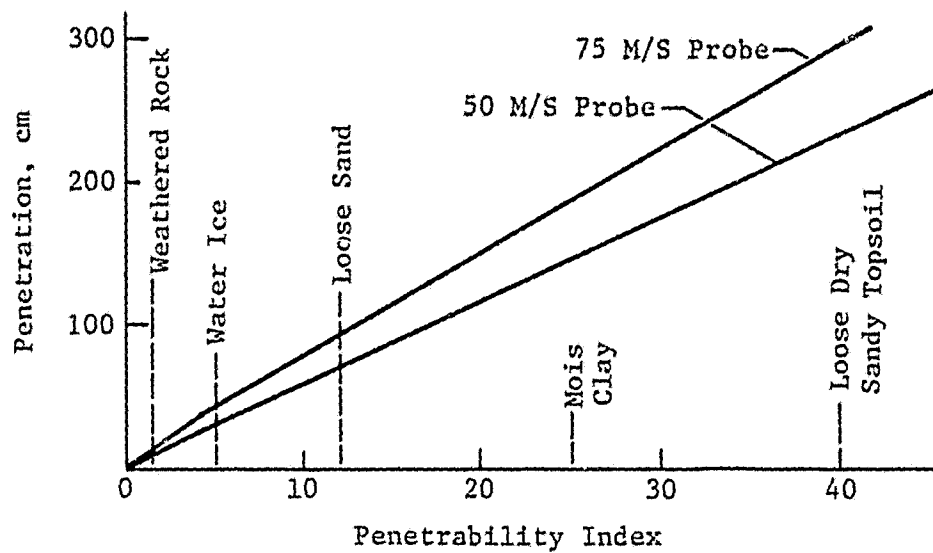


Figure 4.1 Penetration of CNIP into various Surface Materials

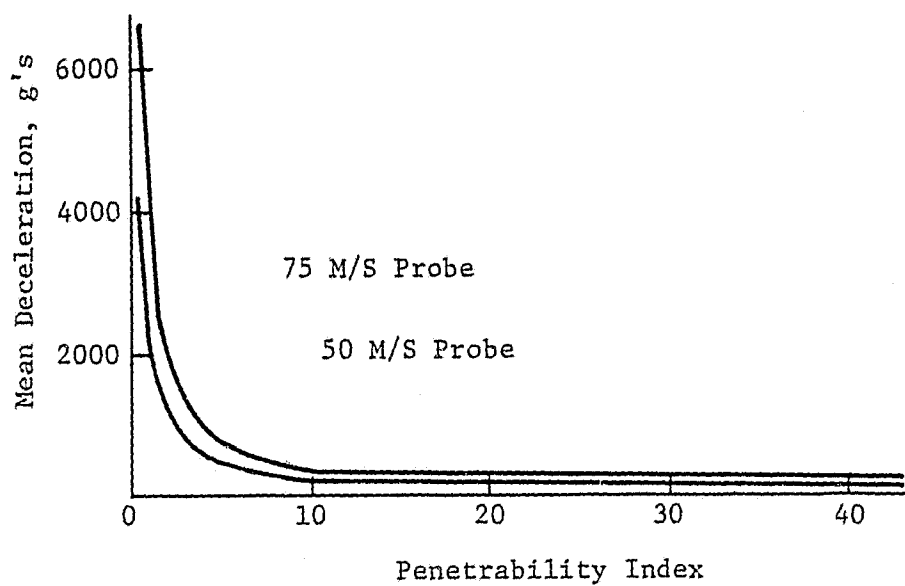


Figure 4.2 Deceleration Experienced by CNIP During Penetration of Various Surface Materials

<u>2.54 cm OD Tubing:</u>	<u>Max g-Level</u>
1/32" Aluminum	4000 g's
1/16" Aluminum	9000 g's
1/32" Steel	13000 g's
1/16" Steel	> 20000 g's

For the purposes of this study the 1/16" Steel tubing was chosen primarily in an attempt to attain a 1 K gram weight.

4.1.3 3. Afterbody - For some penetration scenarios, the afterbody may experience extremely high deceleration. A figure of 20000 g's is mentioned in Ref. 2, and this estimate is used in the study.

It appears that a 20,000 g impact design of the afterbody and braking fins is feasible. However, the design would be simplified if the SRM case did not impact the nucleus with the rest of the CNIP. The probe impact center of gravity could be moved farther forward, and the depth of penetration of the afterbody could be minimized, if the SRM case were separated from the probe. The following for methods can be considered for jettisoning the SRM.

a) Attach the motor such that it is constrained torsionally during firing, but after burnout is forced to separate by means of springs. This would impart a small relative velocity between the probe and the motor section such that the probe arrives at the surface before the motor case. Relative motion between the S/C and nucleus surface is expected to be such that the difference in travel times and other, as yet unidentified, factors would guarantee that the motor not come down on top of the probe. This is an area requiring study.

b) Provide sufficient friction drag on the motor case as it leaves the launch tube so that it is decelerated relative to the probe, resulting in different travel times with similar impact position considerations as given above. This is seen as a less desirable method, in that thrust tailoff after tube exit might close the gap created; as well as that the S/C would experience disturbances.

c) Provide for a means of porting residual thrust after exiting the launch tube, in such a manner that a separation force is applied. This does not appear to be a promising approach, in that it adds to the complexity of the system and may impart a disturbing moment on the probe.

4.1.4 Attitude Stability - In order to facilitate expected probe penetration and correct interpretation of deceleration time histories, a requirement is that at nucleus encounter the probe axis be aligned with the relative velocity vector to within 10° (see Figure 4.3). Because of the passive nature of the probe and a lack of atmosphere to provide aerodynamic stabilization, spin stabilization is the only feasible approach. It is proposed that the necessary spin be imparted by deflecting vanes aft of the rocket motor rather than by rifling in the launch tube. The latter would violate the requirement that the probe experiment not give rise to reaction forces or moments on the S/C, as well as increase the cost and complexity of the equipment.

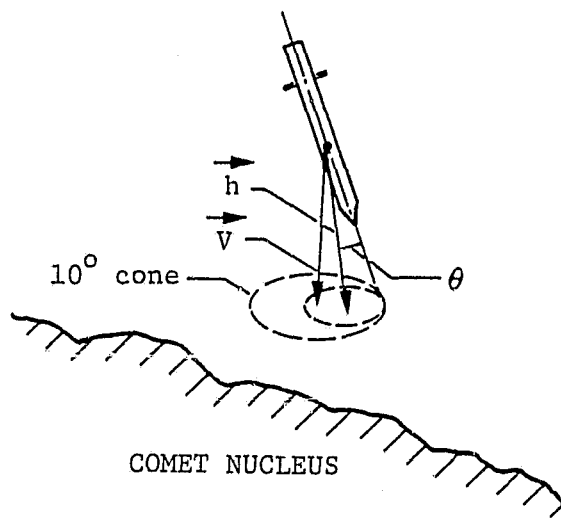


Figure 4.3 - Probe Motion about Velocity Vector

The CNIP configuration is inherently difficult to spin stabilize. In fact, the spin is unstable in the sense that for a given angular momentum, the kinetic energy is much greater if spinning about its longitudinal axis than about a transverse axis. For the CNIP the ratio of moments of inertia about longitudinal and transverse axes is about .006, indicating a strong tendency for an initially longitudinal spin to degenerate into a lateral spin. The low moment of inertia ratio also causes the spinning probe to be affected by disturbing moments at launch and during flight. Figure 4.4 is a plot of the effect on the coning angle of the CNIP of force impulses on the probe.

The angle between the probe spin axis and the velocity vector at impact is determined primarily by four factors:

- a. An impulsive tip-off moment imparted at launch.
- b. Growth of an initially small precession (coning) angle of the probe longitudinal axis during flight to the target.
- c. Flexible body effects.
- d. The inadvertent striking of objects (e.g., debris, pebbles) during flight to the target.

Each of these effects will be considered in the following discussion. Supporting analysis will be found in the Appendix,

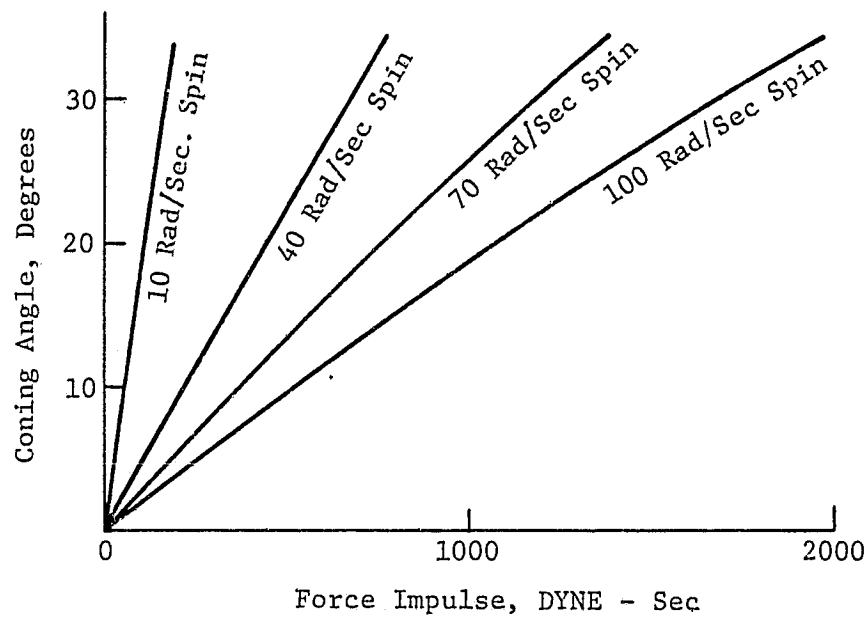


Figure 4.4 Coning Angles Resulting from Lateral Tipoff Forces at Tail of Probe, for Various Probe Spin Velocities

4.1.4.1 Tipoff Moment - A tipoff moment will displace the angular momentum vector \vec{h} from the velocity vector \vec{V} , with the probe then coning about \vec{h} at an angle θ , as is shown in Figure 4.3. The only significant tipoff moment expected is due to misalignment of whatever portion of thrust tailoff occurs after the probe has left the launch tube. Although this cannot be studied in a meaningful way at this time, the nature of its effect can be discussed. The motor thrust characteristics shown in Figure 3.11 indicates that the tailoff would include less than perhaps 1% of the total impulse. Assuming that only 10% of that occurred after probe exit, and that the thrust misalignment is on the order of just 3° , the resulting coning angles for various spin rates of the 75 m/s probes are:

Spin Rate	Coning Angle	PK
20 rad/sec	30°	35°
60 rad/sec	7.9°	13°
100 rad/sec	4.8°	7.9°
APC 200 rad/sec.		4°

It appears that a spin rate below about 60 rad/sec is probably too low to provide the necessary attitude stabilization. The situation may actually be worse than indicated, as the coning takes place about a displaced angular momentum vector. This is an area that will have to be studied before final choice of a rocket motor can be made.

4.1.4.2 Growth of an Initially Small Precession Angle - The precession (coning) rate of the CNIP differs from the spin rate, which results in an excitation of various energy dissipating mechanisms within and on the probe. These include damped structural vibration of the probe body, vibrating loose wires or flexible appendages, sloshing fluid, etc., Figure 4.5 shows the manner in which the coning angle increases as energy is thus lost. It is apparent that a spinning probe coning at a very small initial angle need lose very little energy before the 10° attitude requirement is violated. Fortunately, however, the excitation frequency is very low (≈ 10 Hz) and the amplitude varies with coning angle. Thus, the problem can be avoided by keeping the initial coning angle small and not including such components as a flexible antenna (eg. whip or loose helix).

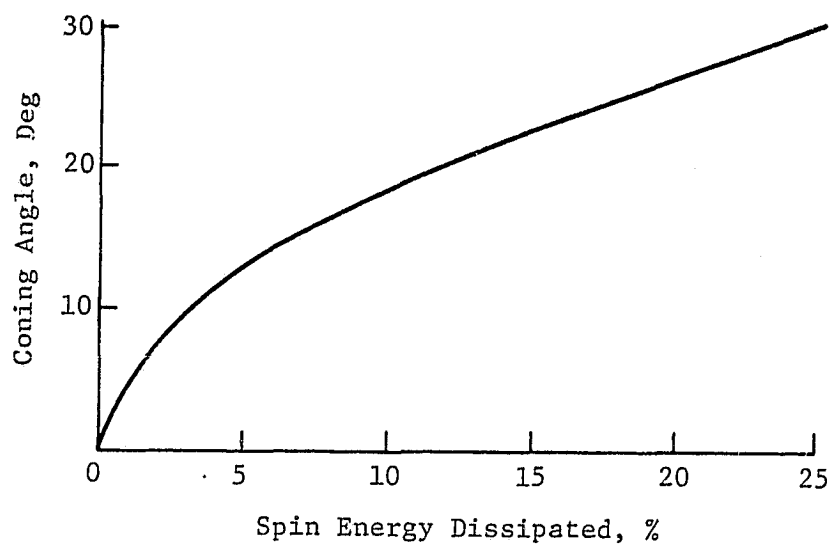


Figure 4.5 Increase in Coning Angle as Spin Energy is Dissipated

4.1.4.3 Flexible Body Effects (Undamped) - Here we are concerned only with a probe configuration which can experience bending deflections in response to the spin such that the probe axis deviates significantly from the longitudinal principal axis of inertia. Because the probe body is quite rigid, this could only occur if some such component as a long whip antenna were deployed. By avoiding such a configuration the problem will not arise.

4.1.4.4 Collision with Objects During Flight - If the CNIP is hit by an object the force impact would affect the probe as shown in Figure 4.4. To illustrate the effect, assume, for example, that the 75 M/S probe strikes a small pebble or rock off the spin axis on the conical nose. If the pebble is at rest relative to the comet nucleus, has a mass of only .1 gram, and the collision is perfectly elastic, the resulting coning angle (which is assumed as zero before the collision) is tabulated below for several spin rates.

<u>Spin Rate</u>	<u>Cone Angle</u>
20 rad/sec	32°
60 rad/sec	12°
100 rad/sec	7°

This example demonstrates the inability of the spin stabilized CNIP to withstand disturbances. It is also apparent that the probe will be able to penetrate very little floating debris before its attitude diverges badly. Some nose shape other than the conical one chosen for this study, could be less sensitive to collision disturbances.

In summary, in order to meet the 10° attitude requirement, the combined effects of the foregoing sources of attitude divergence must be kept as low as possible. To do so the following things should be done:

- o Avoid any significant tipoff moments
- o Spin at as high a rate as is feasible
- o In the design avoid flexible appendages, loose wires, or any other energy dissipating mechanisms.

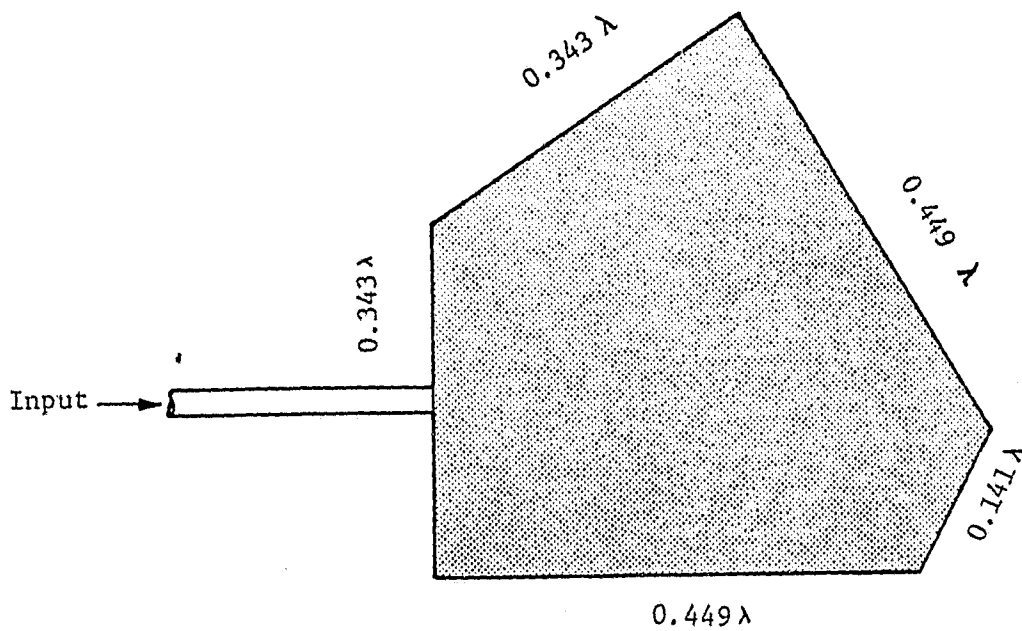
4.2 Alternate CNIP Antenna Concepts Design - Studies
should be conducted to investigate the possibility of implementing an antenna design which will better tolerate the impact shock and be less likely to be buried into the nucleus.

The concept to be considered is to etch an antenna pattern onto a flexible material. The material can then be packaged around the afterbody surface and inflated, like a balloon, when the CNIP exits the launch tube.

Patterns such as the pentagon shape (Figure 4.6) or the Equiangular Spiral (Figure 4.7) can be etched on flexible copper substrate material, such as 3M Company's Epsilon-10. This is bonded on the surface of a compatible plastic material that can be flexible and survive the solid rocket motor environment. A method would be devised to inflate, or expand, the material after the CNIP leaves the launch tube so that the antenna pattern is normal to the long axis of the CNIP. Figure 4.7 contains the deployed antenna.

Care in the design will be required so that the antenna does not affect the spin stability of the probe by imposing disturbing forces to cause coning or despinning.

Typical antenna performance of these antennas are given in Figure 4.6 along with the typical radiation pattern. The disadvantage of the Pentagon Shape Antenna is the limited bandwidth while the Spiral Antenna has an octave bandwidth.



Typical antenna performances are:

Polarization	RHCP or LHCP
Beamwidth (3dB)	86° Nominal
Gain	3 dBi Nominal
Bandwidth	2.5 percent
VSWR	1.5 : 1

Radiation Pattern

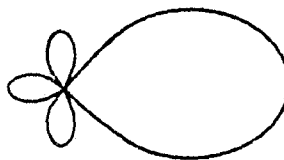


Figure 4.6 Pentagon Shape Microstrip Antenna

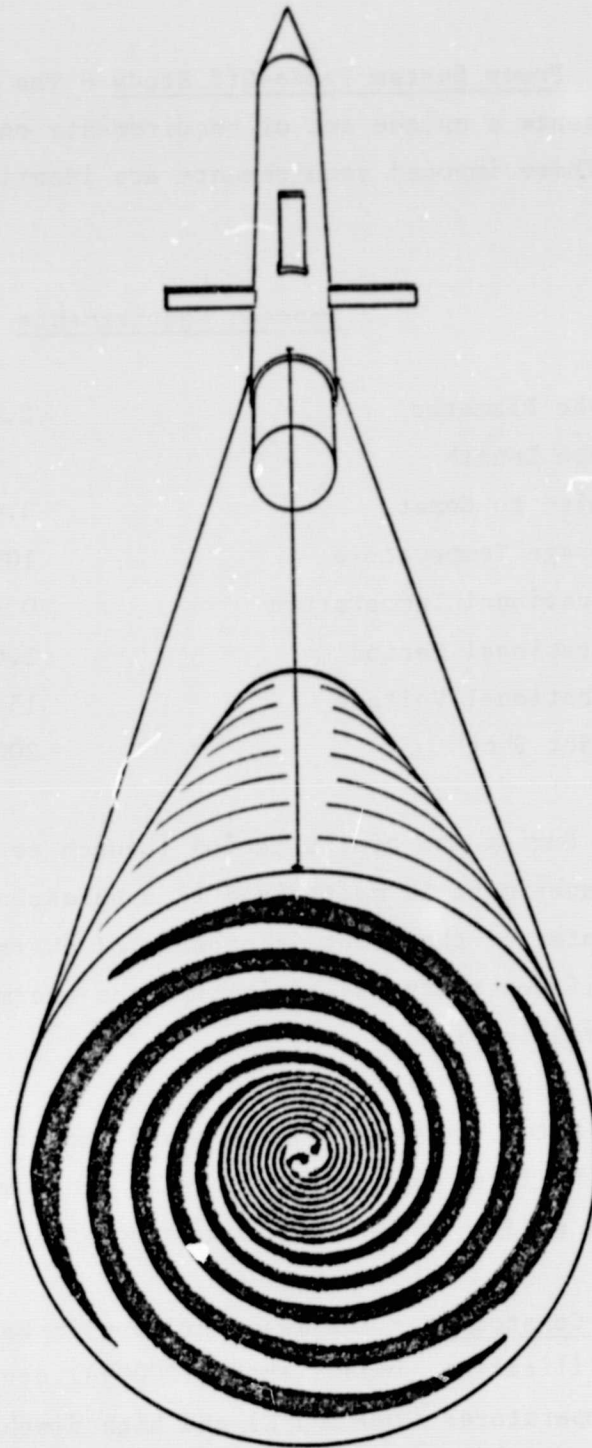


Figure 4.7 Equiangular Spiral Antenna
Deployed from the CNIP

4.3 Power System Trade-Off Study - The Comet Nucleus Impact Probe presents a unique set of requirements on the energy storage system. These imposed requirements are identified in the table below:

Imposed Requirements

Probe Diameter	2.54 cm
Probe Length	40 cm
Cruise to Comet	3.0 yrs.
Storage Temperature	100-300°K
Operational Temperature	0 - 15°C
Operational Period	1.0 hr.
Operational Voltage	15 ± 3 Vdc
Impact Shock	2000 g

During the cruise period (Launch to encounter of comets), the CNIP experiment is maintained in a quiescent state. The orbiter upon encounter of the comet is capable of charging the probe batteries if necessary and activating the thermal blanket for probe thermal stabilization.

After equipment checkout and impact area selection, a probe will be fired into the nucleus of the comet. Probe operational period is defined from launch to 1.0 hours.

Constraint - The major drivers in battery selection are volume sterilization, impact shock (2000g), cruise (up to 3 years), storage temperatures (100-300°K) and high discharge rate.

Energy Cell Evaluated - Three type cells were evaluated for this mission. Nickel cadmium (rechargeable), lithium (primary and reserve) and thermal. The battery characteristics are shown in Table 4.8.

Energy System	CELLS						BATTERY					
	Capacity AH	Dia.	length	Vol IN	Wt. Oz	Balt Vol.	Cells Req.	Dia. in	length	Volume IN ³	Wt. LBS	Comments
LITHIUM (LiSOCl ₂)	0.5	1.0	0.6	0.47	0.77	14.5	5	1.0	3.0	2.36	.24	30 whr/LB
NICKEL CADMIUM	0.25	0.67	0.66	0.24	0.5	15.0	12	1.34	3.96	5.67	.38	10 wh/LB
THERMAL	0.5	0.75	1.75	.19	6.0	15	1	.75	1.75	0.19	.38	Max operation 8.5 min

TABLE 4.8 - Battery System Characteristics

Lithium - The lithium cell is capable of supplying the highest energy density for the comet probe-93 Wh/lb. This could be either a primary or reserve battery. Several technology areas would require investigation if the reserve battery is selected, they are

- o Activation
- o Envelope
- o Long term storage

Use of the Lithium cell would result in a program cost reduction via elimination of a battery charger in the experiment as well as a reduction in the power source (solar array area) reduction of the energy generation and removal of the battery charger would also provide an overall weight reduction.

Nickel Cadmium - The nickel cadmium battery although rechargeable will provide an energy density of 11 Wh/lb, but presents several additional concerns. 1) the Nicad battery in normal operation is a cyclic device and limited data is available on its use in a float or open circuit storage mode. 2) If the battery is flown in the shorted, state additional equipment (shorting switch and resistors) will be required, and 3) charging equipment including umbilical interface between the probe and the Experiment Base Station. Items 2 and 3 would impose additional weight on the systems.

Thermal - The thermal battery is capable of supplying high energy density in excess of 200 Wh/lb but is limited in life. Maximum operational life of a 15-28v thermal battery is 8.5 minutes (510 seconds). Excessive heat generated by the electrolyte/plate interaction would have to be dissipated, thus imposing redesign and additional weight.

Battery Sizing and Selection - Based on an operational period of up to one hour and a volume of 2.37 in³, a battery sizing was made. The current demand for the CNIP from preflight checkout through 1 hour of operation is .8 ampere. Figure 4.8 shows the capacity of the 3 cells at 15 vdc as a function of volume. Included in the sizing are the losses associated with cabling, sterilization and capacity loss as a result of long term storage. The analytical battery sizing is as follows.

Battery Sizing

Energy required	4.3 Whr
Storage Losses	8%
Sterilization Losses	4%
Contingency	1%
Prelaunch Checkout	.2 hrs
Flight	2.3 min
Operational period in Comet	0.5 - 1 Hrs.

Energy required for 1 hour.

$$4.3 \text{ W} \times 1.0 = 4.3 \text{ Whr}$$

$$\frac{\text{whr}}{\text{V}} = \frac{4.3}{15} = .3 \text{ Ahr}$$

$\frac{\text{Ah}}{\text{Losses}} = \frac{\text{Actual battery capacity required at the comet S/C}}{\text{Launch}}$

$$\frac{.3}{(.97)(.96)(.99)} = .33 \text{ Ahr}$$

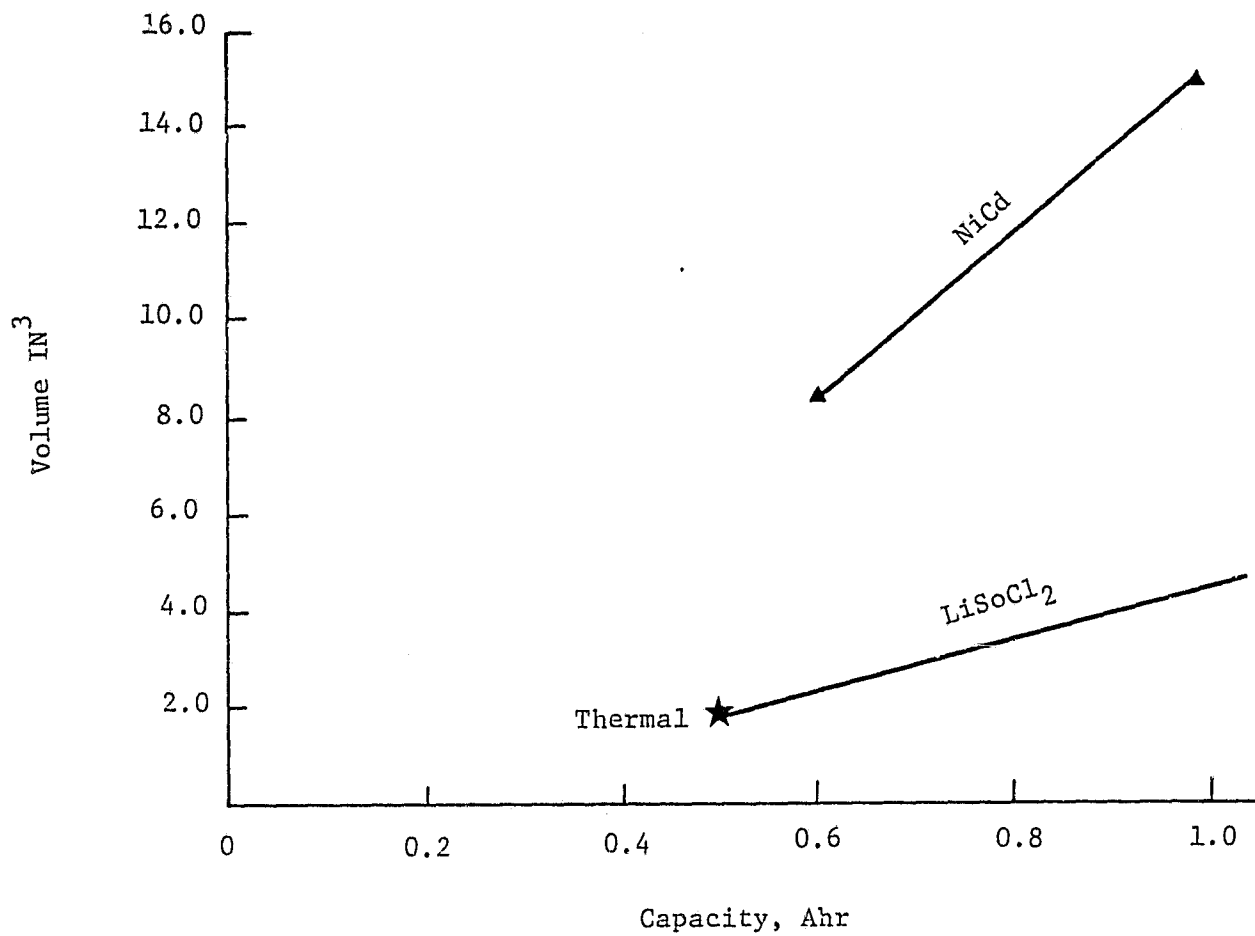


Figure 4.8 Capacity as a function of volume for 3 cells.

5.0 MANAGEMENT

5.1 Program Plan - The program plan for the straw-man CNIP experiment design, is shown in Figure 5.1. It was developed using the following ground rules and assumptions and the Work Breakdown Structure shown in Table 5.1.

a. The CNIP schedule is based on milestones and activity schedules presented in volume IV, Science Management Plan, of the referenced mission document.

b. The CNIP Preliminary Design Review (PDR) and Critical Design Review (CDR) will include simultaneous review of flight hardware, ground support equipment, software and spacecraft interfaces.

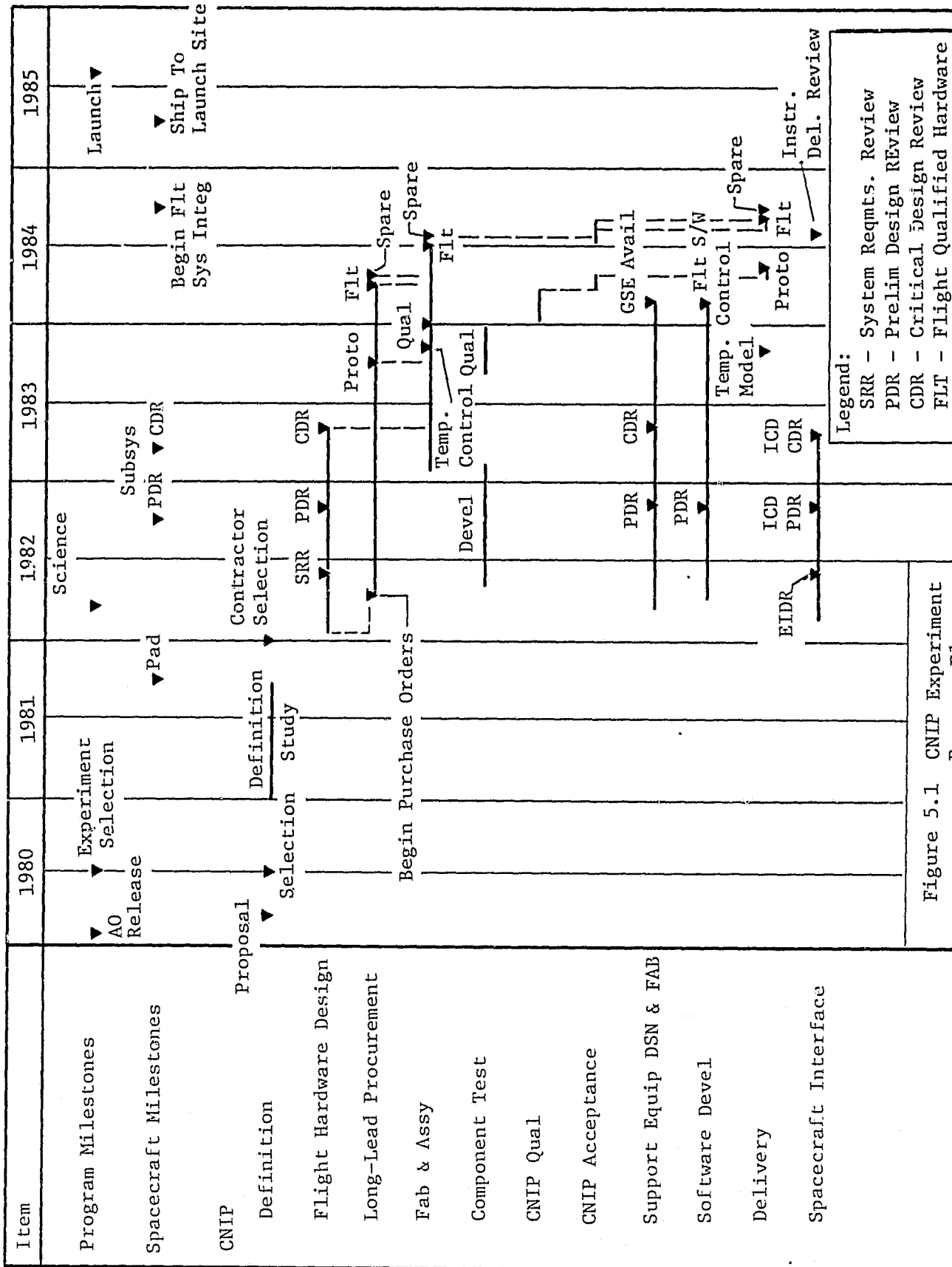
c. The CNIP design reviews follow the spacecraft PDRs and CDRs.

d. Long-lead components will require 24 months after receipt of purchase order for flight qualified hardware delivery. Generally, the kinds of components required for CNIP require no longer than 24 months lead time; however, until further definition of these components is available, a firm lead time is not available. It may require earlier go ahead to vendors that need more than 24 months to deliver, and in turn an earlier project start.

e. The following units will be fabricated and assembled:

	<u>Brass</u>			<u>Science</u>		
	<u>Board</u>	<u>Proto</u>	<u>Qual</u>	<u>Test</u>	<u>Flight</u>	<u>Spare</u>
Tube Assy & Electronics	1	1	1	1	1	1
Probe	1	2	2	3	3	2
AGE					1 Set	

f. All vendor component qualification will be completed prior to flight hardware delivery.



Legend:
 SRR - System Reqmts. Review
 PDR - Prelim Design Review
 CDR - Critical Design Review
 FLT - Flight Qualified Hardware
 ICD - Interface Control Drawing
 S/W - Functional Reqmts Review

Figure 5.1 CNIP Experiment Program Plan

TABLE 5.1
CNIP WORK BREAKDOWN STRUCTURE

	Business Management	Engineering	Manufacturing	Purchase	Test	Software Devel.
1.0 Business Management	X					
2.0 Flight Hardware						
Probes:		X				
Body and Nose			X	X		
Motor				X		
Fins & Mechanism			X			
Accelerometer				X		
Temperature Sensors				X		
Amplifiers				X		
Batteries				X		
Transmitter				X		
Antenna				X		
Tubes		X	X	X		
Thermal Insulation		X		X		
Experiment Base Box		X				
Receiver Electronics			X			
Data Storage				X		
Micro Processor				X		
Command Current				X		
Data Processor Electronics			X			
S/C Interface Circuits			X			
Connectors			X			
Mechanical S/C Interface			X			
3.0 Support Equipment		X				
System Test Set (1)			X	X		
Electrical Test Set (in-line) (2)			X	X		
4.0 Software						X

CNIP WORK BREAKDOWN STRUCTURE

	Business Management	Engineering	Manufacturing	Purchase	Test	Software Devel.	Quality & Reliab.
5.0 Test Program							
Brass Board and Bread Board Engineering Tests					X		
Development							
Concept Verification					X		
Launch Tests					X		
Probe Stability Test					X		
Fin Operation Verification					X		
Antenna Verification					X		
Umbilical Verification					X		
Impact Shock Test					X		
Electronic Design Verification					X		
Thermal Test					X		
Software Test						X	
Qual. Tests (System level)					X		
Environmental							
Thermal Vacuum (Time)					X		
Vibration					X		
Shock/Impact					X		
FMC					X		
Acceptance Tests							
Electrical Ambient					X		
Screening Vibration					X		
Electrical Thermal Vacuum					X		
6.0 FAB & Assembly			X				
7.0 Quality Assur., Reliab.							X

g. The CNIP qualification test may require use of some unqualified components. Only after further specification of CNIP components can we identify which unqualified components will be used. If this approach is an unacceptable risk, it will require earlier go ahead to critical vendors.

h. Support equipment and software are designed and developed in concert with flight hardware.

i. The delivery of the flight qualified units are scheduled to be at the spacecraft contractors one month before the start of spacecraft flight system integration start.

j. The CNIP schedule in this report does not agree with the schedule in Volume II, Management Plan & Cost Plan, CNIP Experiment Proposal, Figure 7. The CNIP experiment development start is six (6) months earlier on the schedule in this report. The prime reason is the 24 month leadtime estimate for parts. Alternate ways to solve this problem are speed up the experiment development contract selection or prepare the long-lead procurement specs during the definition phase and place orders in advance of experiment development start.

5.2 Cost Analysis - A cost analysis was performed for the straw-man CNIP Experiment. The analysis was based on costs experienced in previous programs. These costs were adjusted for differences in functions to be performed and for variations in the complexity of the components. Engineering judgement, and opinions, were used where no direct cost history existed. Using this technique the estimated cost to design, develop, fabricate, test and deliver the CNIP Experiment is estimated to be about \$4.4M. Table 5.2 shows the cost breakdown for this rough order of magnitude estimate.

Page intentionally left blank

TABLE 5.2
 CNIP EXPERIMENT COST BREAKDOWN
 (FOR ENGINEERING USE ONLY)

<u>AREA</u>	<u>ESTIMATED COST</u> (Dollars)
Structure & Mechanism	515 K
Propulsion	277 K
Electronics	277 K
Power	277 K
Telecommunications	277 K
Software	275 K
Test & Fabrication/Assembly	515 K
System Engineering	277 K
 Total Non-recurring Cost	 3.0M
 Parts, Component & Production	 1.0M
 Program Management (@ 10%)	 <u>.4M</u>
TOTAL ROM COST	\$ 4.4M

References

1. NASA, International Comet Mission: 626-2 Vol. II, Mission Description.
2. NASA, International Comet Mission: 626-2 Vol. IV, Science Management Plan.
3. NASA, International Comet Mission: 626-2 Vol. V, Flight System Description.
4. C. W. Young, "Empirical Equations for Predicting Penetration Performance in Layered Earth Materials for Complex Penetrator Configurations". Sandia Laboratories Development Report SC-DR-72 0523, Dec 1972.
5. C. W. Young, L. J. Keck, "An Air Dropped Sea Ice Penetrometer", Sandia Laboratories Development Report SC-DR-71 0729, Dec. 71.
6. W. T. Thomson, "Introduction to Space Dynamics", John Wiley & Sons, 1963.
7. F.W. Hopper, "Active Precession Control for Spin Stabilized Vehicles," AIAA Paper No. 71-952, Aug. 1971.

Page intentionally left blank

APPENDIX

PROBE ROTATIONAL DYNAMICS

The rigid body motion of the symmetric probe during undisturbed flight can be described with reference to the Figure A1, utilizing Euler's Angles. See Ref's 3,4 for analytical details.

The X, Y, Z axes define an inertial frame, with OZ lying along the angular momentum vector \vec{h} . Oz is the probe spin axis, with x and y denoting the two transverse axes. The probe spins at the rate $\dot{\phi}$, and experiences precession of Oz about OZ at the rate $\dot{\psi}$. Let C, A, and A denote the probe moments of inertia about the principal axes Oz, Ox, and Oy respectively. θ denotes the angle of precession or coning of the spin axis about the angular momentum vector.

1. Degradation of Spin with Energy Loss - \vec{h} is ideally aligned with the probe velocity vector \vec{V} during flight, but will be shifted therefrom by tipoff moments at launch or by subsequent collisions with debris, pebbles, etc.

For a given spin situation, angular momentum has a magnitude

$$h = \left\{ A^2 \dot{\psi}^2 \sin^2 \theta + C^2 (\dot{\psi} \cos \theta + \dot{\phi})^2 \right\}^{1/2} \quad (1)$$

and kinetic energy is

$$T = \frac{1}{2} A \dot{\psi}^2 \left(\sin^2 \theta + \frac{A}{C} \cos^2 \theta \right) \quad (2)$$

If in the absence of disturbances, energy is lost through energy dissipating mechanisms that are excited by the precession, an increase in θ is implied by eq. (1). This is accompanied by a change in spin rate $\dot{\phi}$ such that angular momentum, given by Eq. (1), is unchanged. the ratio of spin kinetic energy at any θ to the maximum value (i.e., when $\theta = 0$) is given by the expression

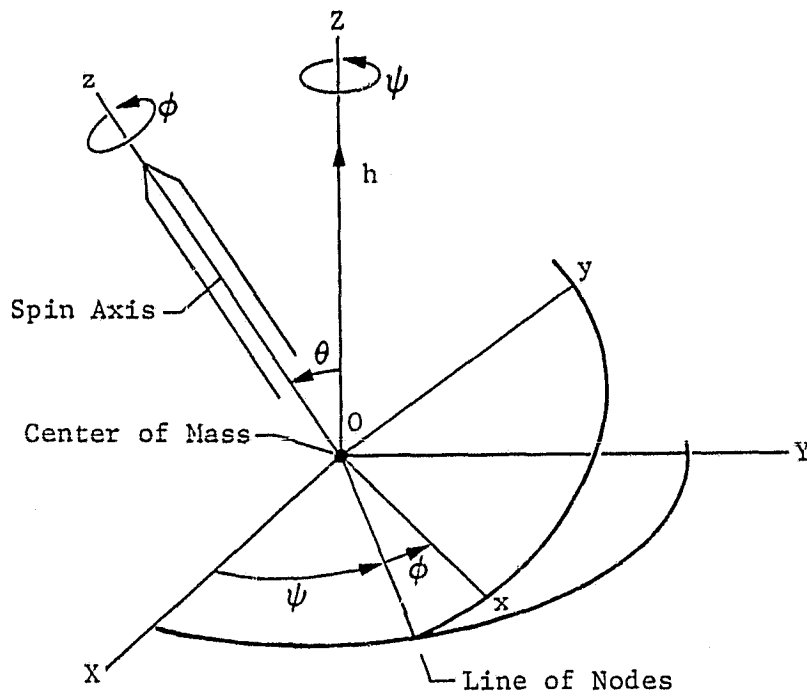


Figure A1. Euler Angle Representation of Spinning Probe

$$\frac{KE}{KE_0} = \frac{C}{A} \sin^2 \theta + \cos^2 \theta \quad (3)$$

Eqn. (3) is the basis of Figure 4.5. As θ approaches 90° , where the spin has degenerated to a rotation about a transverse axis, the ratio approaches $\frac{C}{A}$, which for the CNIP is ~ 0.006 .

(These results also make use of the fact that during such a change in θ at constant \vec{h} , $\dot{\psi} = \frac{h}{A}$, a constant).

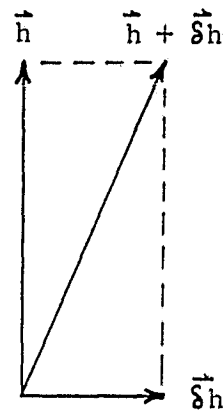
A

2. Response to Disturbing Moments - If the probe is initially spinning with angular momentum \vec{h} and precession angle θ and experiences a moment impulse $\vec{M}\delta t$ about a lateral axis, there results an impulsive change to angular momentum $\vec{\delta h} = \vec{M}\delta t$.

The resultant angular momentum is shifted from the original by the angle $\tan^{-1} \frac{\delta h}{h}$. The probe will now commence

to precess about the displaced angular momentum vector at the same angle, i.e.

$$\theta = \tan^{-1} \frac{\delta h}{h}$$



The long slender CNIP has a small axial moment of inertia, such that for a given spin rate the angular momentum is small. On the other hand, the long moment arm associated with even small disturbing forces produces a large $\vec{\delta h}$, and hence unhappily large precession angles.